Submitted to ApJ

NGC 6791: an exotic open cluster or the nucleus of a tidally disrupted galaxy?

Giovanni Carraro[a,b]

Astronomy Department, Yale University, New Haven, CT 06520−8101, USA

gcarraro@das.uchile.cl

Sandro Villanova

Dipartimento di Astronomia, Università di Padova, Vicolo Osservatorio 2, I−35122, Padova, Italy

villanova@pd.astro.it

Pierre Demarque

Astronomy Department, Yale University, New Haven, CT 06520−8101, USA

demarque@astro.yale.edu

M. Virginia McSwain[c]

Astronomy Department, Yale University, New Haven, CT 06520−8101, USA

mcswain@astro.yale.edu

Giampaolo Piotto

Dipartimento di Astronomia, Università di Padova, Vicolo Osservatorio 2, I−35122, Padova, Italy

piotto@pd.astro.it

and

Luigi R. Bedin

ESO, K. Schwarzschild Str. 2, 85748 Garching, Germany

lbedin@eso.org

ABSTRACT

We report on high resolution Echelle spectroscopy of 20 giant stars in the Galactic old open clusters NGC 6791 obtained with Hydra at the WIYN telescope. High precision radial velocity allow us to isolate 15 *bona fide* cluster members. From 10 of them we derive a global [M/H]=+0.39±0.05. We therefore confirm that NGC 6791 is extremely metal rich, exhibits a few marginally sub-solar abundance ratios, and within the resolution of our spectra does not show evidences of spread in metal abundance. With these new data we re-derive the cluster fundamental parameters suggesting that it is about 8 Gyr old and 4.3 kpc far from the Sun. The combination of its chemical properties, age, position, and Galactic orbit hardly makes NGC 6791 a genuine Population I open cluster. We discuss possible interpretations of the cluster peculiarities suggesting that the cluster might be what remains of a much larger system, whose initial potential well could have been sufficient to produce high metallicity stars, and which has been depopulated by the tidal field of the Galaxy. Alternatively, its current properties may be explained by the perturbation of the Galactic bar on an object originated well inside the solar ring, where the metal enrichment had been very fast.

Subject headings: open clusters: general — open clusters: (NGC 6791)

1. Introduction

NGC 6791 is an extremely interesting and intriguing open cluster. The combination of old age, small distance and high metal abundance makes this cluster very attractive, and indeed in the last 40 years it has been the target of intensive and numerous studies (Carney et al. 2005, and references therein). A large number of optical photometric studies (Stetson et al. 2003 and references therein) has been recently complemented by the deep ACS/HST investigation by King et al. (2005), and the near IR study by Carney et al. (2005).
Since the pioneering study of Kinman (1965) it was clear that NGC 6791 is a very old and very metal rich cluster.

[a]Departamento de Astrónomia, Universidad de Chile, Casilla 36-D, Santiago de Chile, Chile

[b]Andes Fellow, on leave from Dipartimento di Astronomia, Università di Padova, Vicolo Osservatorio 2, I−35122, Padova, Italy

[c]NSF Astronomy and Astrophysic Postdoctoral Fellow

Its age was measured several times by using different sets of isochrones (Carraro et al. 1999 and references therein), and it is probably confined in the range from 8 to 12 Gyr, depending on the cluster precise metal abundance. Taylor (2001, and references therein) critically reviewed all the available metallicity estimates, concluding that the [Fe/H] for NGC 6791 should probably lie in the range +0.16 to +0.44 dex. This combination of age and metallicity is unique in the Milky Way open cluster population, and has been recently questioned by Bedin et al. (2005), whose HST study of the White Dwarf cooling sequence supports a much younger age. As these authors comment, this age discrepancy may arise from defects in the White Dwarf current models, or from the poorly known cluster metal abundance.

Noteworthy, the cluster is also known to harbour a number of sdB/sdO stars (Landsman et al. 1998, Buson et al. 2005), which may be explained by a scenario of a high metallicity driven wind in the Red Giant Branch phase of the progenitors of these stars or, more simply, by the binarity hypothesis (Green et al. 2005) .

The UV upturn (namely the abrupt rise in the UV continuum emission shortward of $\lambda \approx 2000\mathring{A}$) similar to that typical of any ellipical galaxy (Landsman et al. 1998) and the highly eccentric orbit, unusual for a Population I object, contribute to make this cluster even more intriguing .
In an attempt to substantially improve our knowledge of NGC 6791, we carried out a spectroscopic campaign to provide radial velocities and accurate metallicities of a statistically significant number of stars in the cluster. In fact, current abundance determinations either lack sufficient resolution or are restricted to a very small number of stars.
This new set of abundance estimates coupled with the high quality of existing photometry (Stetson et al 2003) allow us to significantly improve on the fundametal parameters of this cluster, and better clarify its intriguing nature.

2. Observations

The observations were carried out on the night of July 28, 2005 with the Hydra spectrograph at the WIYN telescope at Kitt Peak observatory under photometric conditions and typical seeing of $1\farcs1$ arcsec. The MOS consists of the Hydra positioner, which in 20 minutes can place 89 fibers within the 1-degree diameter focal plane of the telescope to ≈ 0.2 arcsec precision. This project employed the 3-arcsec diameter red-optimized fiber bundle. The fibers feed a bench-mounted spectrograph in a thermally isolated room. With the echelle grating and Bench Spectrograph Camera the system produces a resolution of 20,000 at 6000

Å . The wavelength coverage of 200 Å around the central wavelength of 6000 Å provides a rich array of narrow absorption lines. We observed 20 RGB/clump stars with 45 min exposures, for a grand total of 4.5 hours of actual photon collection time on the same single star. The 20 stars where selected from the Stetson et al. (2003) photometric catalog to be giant stars and to have the right magnitudes to be observed with the WIYN 3.6m telecope. We restricted the sample to giant stars brighter than V $\approx$ 15. The stars are listed in Table 1, where first column reports Stetson et al. (2003) numbering and column 2 Kinman (1965) numbering (K65). Then coordinates, magnitudes and colors are taken from Stetson et al. (2003). The radial velocities and spectral classification have been derived in this paper, following Villanova et al. (2004).

3. Data Reduction

Images were reduced using IRAF[2], including bias subtraction, flat-field correction, frame combination, extraction of spectral orders, wavelength calibration, sky subtraction and spectral rectification. The single orders were merged into a single spectrum. As an example, we show in Figure 2 a portion of the reduced, normalized spectrum for star #11814 where some spectral lines are identified. Some spectra have very low S/N, although all the observed stars have practically the same magnitude. This could happen for two reasons: the first one is an imperfect pointing of the fiber and the second one a possible bad fiber-trasmission. Because of this, we could not use five stars for abundance measurements (see below).

4. Radial Velocities

Radial velocities (RV) for RGB and clump stars in NGC 6791 have been determined many times in the past. Kinman (1965) obtained radial velocities for 19 stars, and spectral type for 21. Later, RVs have been measured by Geisler (1988, 12 stars), Friel et al. (1989, 9 stars), Garnavich et al. (1994, 18 stars), Scott et al. (1995, 32 stars) and Friel et al. (2002, 41 stars), with different resolution and precision.

We derived here RVs for 20 stars (see Table 1). The radial velocities of the target stars were measured using the IRAF FXCOR task, which cross-correlates the object spectrum with a

[2]IRAF is distributed by the National Optical Astronomy Observatories, which are operated by the Association of Universities for Research in Astronomy, Inc., under cooperative agreement with the National Science Foundation.

template. As template, we used a synthetic spectrum calculated by SPECTRUM (see 5.2 for a description of the program) with roughly the same atmospheric parameters and metallicity of the observed stars. The final error in the radial velocities was typically less than 0.2 km s^{-1}, and in many cases less than 0.1 km s^{-1}. These errors are significantly lower than in any other previous investigation. This allowed us to clean out field interlopers and isolate 15 *bona fide* members. RVs are plotted in Figure 3. Five stars have radial velocites completely different from the others, and so were considered non-members, although it possible that some of them are binary stars.

A few of our targets are in common with previous investigations, and we can have an external check on our RV measurements. For 11 stars we provide the first estimate of the RV.

In general, we find that Garnavich et al. (1994) RV estimates (for stars 3003, 3010, 3036, 2001, 3018 and 2008) are systematically larger than ours, by about 5-7 km s^{-1}, although, given their typical large error (5 to 15 km/sec), these differences cannot be considered statistically significant. Also Kinman (1965) RVs for the two stars in common with our investigation (stars 2001 and 2008) are larger than our estimate. The largest deviation is with respect to the RVs by Friel et al. (2002), and their previous measurements (Scott et al. 1995, Friel et al. 1989). In this case, there are differences in some case exceeding 20 km s^{-1} (stars 3003 and 2008). Finally, within the errors, we find a good agreement for the two stars (stars 3003 and 3010) we have in common with Geisler (1988).

From the RVs of the 15 cluster members in our sample, we obtain a mean radial velocity $V_r = -47.1 \pm 0.8$ km s^{-1}, in good agreement, within the errors, with the values obtained by the other authors, with the exception of Kinman (1965). The RV dispersion results to be $\sigma_r = 2.2 \pm 0.4$ km s^{-1}.

5. ABUNDANCE ANALYSIS

5.1. Atmospheric parameters

The atmospheric parameters were obtained from the photometric BVI_C data of Stetson et al. (2003). According to Stetson et al., the most likely reddening and absolute distance modulus are E(B-V) = 0.09 [(E(V-I) = 0.11)] and $(m - M)_0 = 12.79$. Effective temperatures (T_{eff}) were obtained from the color-T_{eff} relations of Alonso et al. (1999), Sekiguchi & Fukugita (2000), and Ramirez & Melendez (2005). The temperatures, obtained from the B-V and V-I colors using the quoted relations, are in agreement within 50-100 ^0K. The gravity log(g) was derived from the canonical formula :

$log(\frac{g}{g_\odot}) = 4 \times log(\frac{T_{eff}}{T_\odot}) - log(\frac{L}{L_\odot}) + log(\frac{M}{M_\odot})$

In this equation, the mass $M/M_\odot$ was derived from Straizys & Kuriliene (1981). The lumi-

nosity $L/L_{\odot}$ was derived from the absolute magnitude M_V, adopting the distance modulus of Stetson et al. (2003). The bolometric correction (BC) was derived from the BC-T_{eff} relation from Alonso et al. (1999). The typical error in log(g) is 0.1 dex.
Finally, the adopted microturbulence velocity is the mean of the values given by the relation (Gratton et al. 1996):
$v_t = (1.19 \times 10^{-3})T_{eff} - 0.90log(g) - 2$;
and the relation (Houdashelt et al. 2000):
$v_t = 2.22 - 0.322log(g)$.
The typical error in v_t is 0.1 kms^{-1}.

5.2. Abundance determination

The resolution (R=17,000 at 6580Å) of our spectra, the high metallicity of the cluster, and the low temperature of the target stars cause a lot of blending, and therefore it was not possible to measure the equivalent width of the single spectral lines. For this reason, the abundances were determinated by comparing the observed spectra with synthetic ones. The synthetic spectra were calculated by running SPECTRUM, the Local Thermodynamical Equilibrium (LTE) spectral synthesis program freely distributed by Richard O. Gray (see Piotto et al. 2005 for the details on our synthetic spectra calculation). Model atmospheres were interpolated from the grid of Kurucz (1992) models by using the values of T_{eff} and log(g) determined as explained in Section 5.1. We analized stars with $T_{eff} > 3900^0K$ because, for lower temperatures, molecular bands were present, creating difficulties for continuum determination. We could analyze only ten stars, after rejecting the non-members and the stars which resulted to be too faint and too cool.

First of all, we compared the entire spectrum (range 6400-6760 Å) with the synthethic one in order to obtain an estimate od the global metallicity [M/H]. Then, we analized single lines in order to measure abundances of Fe, Ca, Ti, Ba, Al, Ni, and Si.

A preliminary lines-list was obtained considering all the strongest lines present in our spectra, identified using the line-list distributed with SPECTRUM. The final lines-list was created from the preliminary one by comparing the observed solar spectrum with a sinthetic one, calculated with SPECTRUM for the Sun parameters ($T_{eff} = 5777K, log(g) = 4.44, v_t = 0.8m/s$). The lines in the synthetic spectrum which did not properly match the observed ones were rejected. We also checked whether the preliminary line identification was correct using the MOORE line database (Moore et al. 1966). Table 3 shows the final list of lines we used in our analysis. The resulting metallicities for each star are listed in Table 4.

Due to the radial velocity shit, a few lines (6462.567, 6475.630, 6493.781, 6532.890 Å) overlapped with telluric lines. We did not consider these lines in the abundances determination.

An example of the comparison between synthetic and observed spectra is shown in Fig. 4, for the case of star #11814 Finally, using the stellar parameters [colors, T_{eff}, and log(g)] and the absolute calibration of the MK system (Straizys & Kuriliene 1981), for each star, we derived the stellar spectral classification (see Villanova et al. 2004 for details), which is listed in Col. 9 of Table 1.

The weighted mean of the [Fe/H] content of the ten members of NGC 6791 analysed in the present paper is [Fe/H] = +0.39±0.01 (internal error). Previous investigations reported a variety of estimates for the metallicity of NGC 6791. By using low resolution spectroscopy, Friel & Janes (1993) obtained [Fe/H] = +0.19±0.19 from 9 stars, and Friel et al. (2002) [Fe/H] = +0.11±0.10 from moderate resolution spectra of 39 stars. Because of the large errors, the first estimate is compatible with our one, within one sigma, while the second one is off by almost 3σ.

Interestingly enough, our results are in very good agreement with the study by Peterson & Green (1998), who derived [Fe/H] = +0.40±0.10 for star #2017, a cool blue horizontal branch star, using a resolution very similar to the one used in the present study.

In conclusion, our results confirm that NGC 6791 is actually a very metal rich cluster. Noteworthy, within the errors of our measurements, the metallicities listed in Table 4 do not show any significant abundance spread.

5.3. Abundance ratios

Abundance ratios constitute a powerful tool to assign a cluster to a stellar population (Friel et al. 2003, Carraro et al. 2004, Villanova et al. 2005).
In Table 5 we list the abundance ratios for the observed stars in NGC 6791. These values do not show any particular anomaly. All the abundance ratios are solar scaled, with the only exception of [Al/Fe] and [Ba/Fe], which seem to be slighlty under-abundant. Our ratios are in good agreement with those provided by Peterson & Green (1998).

6. Distance and age of NGC 6791

Our accurate determination of the metal content of NGC 6791 allows a new, more reliable estimate of the cluster distance and age.
To this purpose, in this section, we are going to fit the observed Color Magnitude Diagram (CMD) from Stetson et al. (2003) with both the Padova (Girardi et al. 2000) and Yale-Yonsei isochrones (Yi et al. 2001; Demarque et al. 2003). Previous similar studies allowed to confine the cluster age in the relatively large interval between 8 and 12 Gyrs (Carraro et al. 1994, Chaboyer et al. 1999, King et al. 2005, Carney et al. 2005, and reference therein). As discussed in Stetson et al (2003), and confirmed in this work, the cluster reddening is E(B-V) = 0.09±0.04. There is a large scatter in the literature on the absolute distance modulus $(m - M)_o$ estimates, which range in the interval between 12.6 and 13.6. These large uncertainties in both age and distance have been usually ascribed to uncertainties in the cluster metal abundance. The new specroscopic data presented in this paper allow to put on a more solid basis these fundamental parameters.

6.1. Padova Isochrones

Our [Fe/H] = 0.39 empirical measurement, translates into a metallicity Z = 0.046 (Carraro et al. 1999) and implies a $\Delta Y/\Delta Z$ close to 2. We generated isochrones for this metallicity, and for ages ranging from 7 to 11 Gyrs from Girardi et al. (2000). An appropriate and meaningful isochrone fit implies that all the loci of the CMD, e.g. the turn-off point (TO), the sub giant branch (SGB), the red giant branch (RGB), and the clump of He-burning stars must be simultaneously overlapped by the models. Our best fit (by eye) estimate is shown in Fig. 5 and 6, both in the V vs (B-V) and V vs (V-I) plane. In Fig. 5 we plot the V vs (B-V) CMD of NGC 6791, and superpose the whole set of isochrones, whereas, in Fig. 6, we only show the best fit isochrone in the V vs (B-V) and V vs (V-I) plane.

The isochrone solutions in Fig. 5 have been obtained by shifting the theoretical lines by $E(B - V) = 0.09$ and $(m - M)_V = 13.35$. Clearly ages older than 9 Gyr can be ruled out, since a fit to the TO with an older isochrones implies to decrease the distance modulus, but, in this way, the theoretical clump would be brighter than the observed one. On the other hand, also ages younger than 8 Gyr do not seem possible, since a fit of the TO region with a younger isochrone would result in a RGB redder than the observed one (impling a reddening value significantly larger that the observational limits), and also the clump magnitude would be fainter than the observed counterpart.

Only the isochrones for ages of 8 and 9 Gyr provide a good fit. In details, the 9 Gyr

isochrone fits well the CMD with the adopted parameters, although the clump luminosity turns out to be slightly brighter than the observed one. On the other hand, the 8 Gyr isochrone must be shifted by $E(B-V) = 0.09$ and $(m-M)_V = 13.45$ to provide a very good fit. This is shown in Fig. 6. We note that the lower MS is mismatched. This is a well known problem for metal rich clusters, as extensively discussed by Bedin et al. (2001), and it is likely due to problems in the transformation of the models from the theoretical to the observational plane.

On the overall, however, the fit is very good, and implies for NGC 6791 this set of fundamental parameters: 8.0±1.0 Gyr, 13.07±0.05 (internal error), and 0.09±0.01 for the age, absolute distance modulus, and reddening, respectively. The associated errors are internal errors and have been estimated by eye. They simply reflect the degree of freedom we have to displace the isochrones, still achieving an acceptable fit.

6.2. Yale-Yonsei Isochrones

An independent determination of the age, distance, and a constraint on the reddening of NGC 6791 can be derived using the Y^2 isochrones (Yi et al. 2001; Demarque et al. 2003). The Padova and Y^2 isochrones were both constructed using the same OPAL opacities tables. Otherwise, the description of the microscopic and macroscopic physics, as well as the numerical procedures, differ in many details in the two sets of isochrones. The color transformations are also independently derived.

In the Y^2 system, in which $Z_\odot = 0.0181$, [Fe/H] = 0.39 corresponds to $(Y, Z) = (0.31, 0.04)$. The fit is based on the main sequence (MS) position just below the TO, the position of the TO point, the SGB, and the RGB color. A good fit, as shown in Fig. 7, is obtained for $(m-M)_V = 13.35$, 0.1 mag smaller than the distance modulus we used for the Padova isochrone fit. The best fit is obtained by assuming a reddening $E(B-V) = 0.13$, somewhat larger than the reddening adopted in the previous section, but still within the estimated range of previous investigations. The age we derive from the Y^2 fit is between 8 and 9 Gyr, in good agreement with the Padova age, even though one notes that the position of the lower main sequence differs in the two sets of isochrones. The unevolved main sequence of the Padova isochrones has a steeper downward slope than the observations, whereas the opposite holds for the Y^2 isochrones.

Similarly, Chaboyer et al. (1999) conclude that the cluster age is 8.0 ± 0.5 Gyr, assuming [Fe/H] = 0.4, but using an older observational data set (Kaluzny & Rucinski 1995), and a version of the Yale stellar evolution code that slightly differs from the one used to construct

the Y^2 isochrones. In an analysis of their infrared photometry, Carney et al. (2005) derive an age between 9 Gyr (for [Fe/H] = 0.3) and 7.5 Gyr (for [Fe/H] = 0.5), also in good agreement with our result. Both the Chaboyer et al. (1999) and the Carney et al. (2005) ages are consistent with the Padova and Y^2 fits described in this paper. We should note however that the Carney age estimates were obtained using the same set of Y^2 isochrones that we used in the present work, and therefore their age determination is not completely independent form our one.

Stetson et al. (2003) derive a much older age (12 Gyr) with the help of unpublished VandenBerg isochrones. It appears that the large difference in age is due in part to the authors' choice of a markedly smaller absolute distance modulus (12.79 mag). A superposition of the Y^2 isochrones for the range 8-12 Gyr, shifted by $(m - M)_0 = 12.79$ and $E(B - V) = 0.09$ (Stetson et al. adopted values), on the CMD of NGC 6791 is shown in Fig. 8, for comparison purpose. Although it is not possible to rule out completely the Stetson et al. (2003) fit, the disagreement with other well calibrated isochrones raises questions about the calibration of the VandenBerg isochrones.

An additional, independent age and distance estimate is in King et al. (2005) who obtained an excellent fit of the upper main sequence, TO, and SGB both of Stetson et al. (2003) groundbased CMD of NGC 6791, and of their ACS/HST CMD in the F606W, F814W bands by using the Teramo isochrone set by Pietrinferni et al. (2004). From both fits, King et al. (2005) derived an age of 9 ± 1 Gyr, an absolute distance modulus $(m - M)_0 = 13.0$, and a reddening E(B-V)=0.12 for a metallicity [M/H]=+0.4, and Y=0.288. Also in the fit of the $m_{\rm F814W}$ vs. $m_{\rm F606W}$-$m_{\rm F814W}$ ACS/HST CMD, the Teramo isochrones tends to be redder and redder going to fainter magnitudes, starting from $\sim$ 2 magnitudes below the TO, as already noticed for the Padova isochrones.

Finally, we must mention that the precise age of NGC 6791 also depends on the adopted value of the ratio $(\Delta Y/\Delta Z)$ for galactic helium enrichment. This quantity is poorly known; it may be a function of Z, and may differ from system to system. Demarque et al. (1992) have found that varying Y from 0.32 to 0.36 could reduce the age of the cluster by as much as 15%. The age estimate of NGC 6791 might have to be increased if the enrichment ratio $\Delta Y/\Delta Z$ is much less than 2 (isochrones for $\Delta Y/\Delta Z$ near 2 were assumed in the Padova, Y^2, Teramo, and VandenBerg fits).

With our present knowledge of the $\Delta Y/\Delta Z$ parameter, we conclude that the age of NGC 6791 must be in of range 7.5-8.5 Gyr, with a higher preference towards the higher limits. We point out that, even in the unlikely event that the age of NGC 6791 is as low as 7.5 Gyr, its high metallicity and age present a major challenge to the accepted view of Galactic chemical enrichment.

In conclusion, three sets of independent isochrones consistently inply that the age of NGC 6791 is around 8 Gyr, adopting the metallicity and the reddening coming from observations. The difference in reddening might simply ascribed to the different Helium abundance adopted, and to some photometric zero point error.

7. DISCUSSION and CONCLUSIONS

The hardest point with NGC 6791 is how inside this cluster such high metallicity stars could have been produced. In fact, this cluster does not have any counterpart in the Milky Way. We note here that Kinman (1965) originally identified NGC 6791 as a globular cluster. Even if this interpretation were to be adopted, the high metallicity of NGC 6791, much higher than that of any Galactic globular cluster or nearby dwarf galaxy, remains mysterious.

With Berkeley 17 and Collinder 261, NGC 6791 is one of the oldest open clusters of the Galaxy (Carraro et al. 1999), but its metal abundance is incomparably higher. Moroever, NGC 6791 is one of the most massive open clusters (4000 $M_{\odot}$ at least). It lies at 1 kpc above the Galactic plane, inside the solar ring. This combination of mass and position is hard to explain, since the interaction with the dense Galactic environment should strongly depopulate a typical open cluster.

NGC 6791 is routinely considered in the studies of the chemical evolution of the Galactic disk, and occupies a unique position in the Galactic disk radial abundance gradient (see Fig. 9). By including NGC 6791, the slope of the gradient changes from -0.05 (solid line) to -0.07 (dashed line). Besides, if one considers the slope defined only by clusters older than 4 Gyr (Friel et al. 2002, Fig. 3, upper panel), the slope doubles, from -0.06 to -0.11.
In the same figure, the horizontal solid line indicates the epicyclical amplitude of NGC 6791 orbit (see below, and Carraro & Chiosi 1994). One can readily see how NGC 6791 is quite an exotic object. If, by chance, at the present time the cluster would be at different orbit phase, which would put it, e.g., beyond 12 kpc, there would be a drastic change and even an inversion of the slope of the Galactic disk abundance gradient. Finally, the position of this cluster in the Galactic disk Age-Metallicity relationship (Carraro et al. 1998) is puzzling as well, since the cluster significantly deviates from the mean trend.

In Fig 10 we present NGC 6791 Galactic orbit. This was obtained by integrating back

in time (1 Gyr) the cluster from its present position and kinematics using the Galaxy N-body/gasdynamical model by Fux (1997, 1999). The adopted radial velocity and proper motions come from Geisler (1988) and Cudworth (private comunication), whereas the Galactocentric rectangular initial conditions (positions and velocities) was derived as in Carraro & Chiosi (1994).
Intererstingly enough, this plot shows that the cluster moves from the outer disk regions of the Milky Way, more than 20 kpc far away from the Galactic center, and enters the Solar Ring going as close as 6 kpc from the Galactic center.

The eccentricity (e=0.59) of this orbit is quite high for a Population I star cluster (Carraro & Chiosi 1994), and it is much more similar to a globular cluster/dwarf galaxy orbit.

A plausible scenario is that NGC 6791 is what remains (the nucleus) of a much larger system, which underwent strong tidal disruption. This would explain the cluster orbit, and provide a reasonable explanation for the high metallicity of its stars, which could have been produced only inside a deep potential well.

However, within the observational errors, we did not find any significant abundance spread. This would mean that the bulk of the stars in the cluster was produced in a single burst of star formation. This fact makes more difficult the capture interpretation since Local Group Galaxies normally exhibit spreads in metal content and possess lower metal abundance (Mateo 1998). We stress however the fact that our results are based on only ten stars, and that only larger spectroscopic surveys can better address this particular problem.

An alternative more conservative scenario is that the cluster was born in the inner side of the Galaxy, close to the bulge, where the metal enrichment has been fast. Grenon (1999) studied the kinematics of a group of old (10 Gyrs) metal rich $[M/H] \geq 0.30$ stars and suggested that they formed close to the bulge and then migrated at large Galactocentric distance due to the perturbation of the Galactic bar.

The orbit we calculated actually includs the effect of the bar, and NGC 6791 indeed moves well outside the solar circle. NGC 6791 is very concentrated for an open cluster, and spent most of its time at moderate Galactic latitude. This might help to explain its survival.

The observations described in this paper were carried out remotely from Yale University by Giovanni Carraro. We deeply acknowledge Diane Harmer, George Will and Chris Hunter for support and help. The work of GC is supported by *Fundacion Andes*. GP and SV

acknowledge the support by the italian MIUR, under the program PRIN2003. MVM is supported by an NSF Astronomy and Astrophysics Postdoctoral Fellowship under award AST−04011460. PD's research is supported in part by NASA grant NAG5-13299.

REFERENCES

Alonso A., Arribas S., Martínez-Roger C. 1999, A&A 140, 261

Anders E., Grevesse N. 1989, GeCoA 53, 197

Bedin L.R., Anderson J., King I.R., Piotto G. 2001, ApJ 560, L75

Bedin L.R., Salaris M., Piotto G., King, I.R., Anderson J., Cassisi S., Momany Y. 2005, ApJ 624, L45

Buson L.M., Bertone E., Buzzoni A., Carraro G. 2005, Baltic Astronomy , in press (astro-ph/0509772)

Carney B.W., Lee J.-W., Dodson B. 2005, AJ 129, 656

Carraro G. & Chiosi C. 1994, A&A 288, 751

Carraro G., Chiosi C., Bertelli G., Bressan A. 1994, A&AS 103, 375

Carraro G., Ng Y.K., Portinari L. 1998, MNRAS 296, 1045

Carraro G., Girardi L., Chiosi C. 1999, MNRAS 309, 430

Carraro G., Bresolin F., Villanova S., Matteucci F., Patat F., Romaniello M. 2004, AJ 128, 1676

Chaboyer B., Green E.M., Liebert J. 1999, AJ 117, 1360

Demarque P., Green E.M., Guenther, D.B. 1992, AJ 103, 151

Demarque P., Woo J.-H., Kim Y.C., Yi, S. 2004, ApJS, 155, 667

Friel E.D., Janes K.A. 1993, A&A 267, 75

Friel E.D., Liu T., Janes K.A. 1989, PASP 101, 1112

Friel E.D., Janes K.A., Tavarez M., Jennifer S., Katsanis R., Lotz J., Hong L., Miller N. 2002, AJ 124, 2693

Friel E.D., Jacobson H.R., Barrett E., Fullton L., Balachandran A.C., Pilachowski C.A. 2003, AJ 126, 2372

Fux R. 1997, A&A 327, 983

Fux R. 1999, A&A 345, 787

Garnavich P.M., Vandenberg D.A., Zurek D.R., Hesser J.E. 1994, AJ 107, 1097

Geisler D. 1988, PASP 100, 338

Girardi L., Bressan A., Bertelli G., Chiosi C. 2000, A&AS 141, 371

Gratton R.G., Carretta E., Castelli F. 1996, A&A 314, 191

Green E.M., For B.-Q., Hyde E.A. 2005, in Proc. 14th European Workshop on White Dwarfs, held at Kiel, July 19-23, 2004, ASP Conf. Ser. Vol. 334, eds. D. Koester, S. Moeller (San Francisco: ASP)

Grenon M. 1999 Ap&SS 254, 331

Kaluzny J., Rucinski S.M. 1995, A&AS 114, 1

King. I.R., Bedin L.R., Piotto G., Cassisi S., Anderson J. 2005, AJ130, 626

Kinman T.D., 1965, ApJ 142, 655

Kurucz R.L. 1992, in IAU Symposium 149, The Stellar Populations of Galaxies, ed. B. Barbuy & A. Renzini (Dordrecht:Kluwer), 225

Landsman W., Bolihn R.C., Neff S.G., O'Connell R.W., Roberts M.S., Smith A.M., Stecher T.P. 1998, AJ 116, 789

Mateo M. 1998, ARA&A 36, 435

Moore C.E., Minnaert M.G.J., Houtgast J. 1996, The solar spectrum from 2935 to 8770 Å , United States Department of Commerce, National Bureau of Standards.

Peterson R., Green E.M. 1998, ApJ 502, L39

Pietrinferni, A., Cassisi, S., Salaris, M., and Castelli, F., 2004, ApJ 612, 168.

Piotto G., Villanova S., Bedin L.R., Gratton R., Cassisi S., Momany Y., Recio-Blanco A., Lucatello S., Anderson J., King I.R., Pietrinferni A., Carraro G., ApJ 621, 777

Ramirez I. & Melendez J. 2005, ApJ 626,465

Scott J.E., Friel E.D., Janes K.A. 1995, AJ 109, 1706

Sekiguchi M. & Fukugita M. 2000, AJ 120, 1072

Stetson P.B., Bruntt H., Grundahl F. 2003, PASP 115, 413

Straizys V., Kuriliene G. 1981, Ap&SS 80, 353

Taylor B.J. 2001, A&A 377, 473

Villanova S., Baume G., Carraro G., Geminale A. 2004, A&A 419, 149

Villanova S., Carraro G., Bresolin F., Patat F. 2005, AJ 130, 652

Yi S., Demarque P., Kim, Y.-C., Lee Y.-W., Ree C.H., Lejeune Th., Barnes S. 2001, ApJS, 136, 417

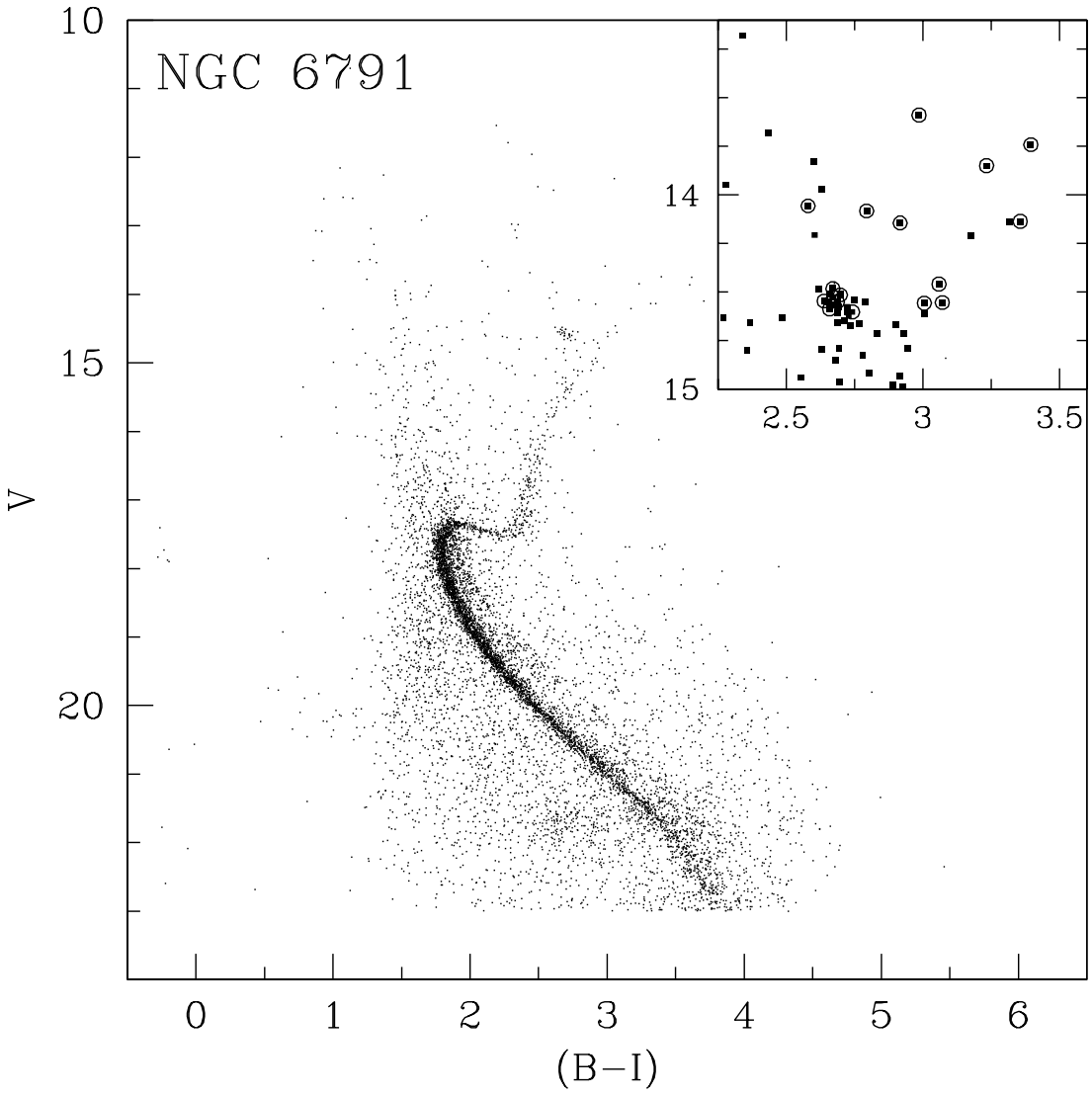

Fig. 1.— The CMD of NGC 6791 (from Stetson et al. 2003 photometry). The upper right inset shows the position of the observed stars.

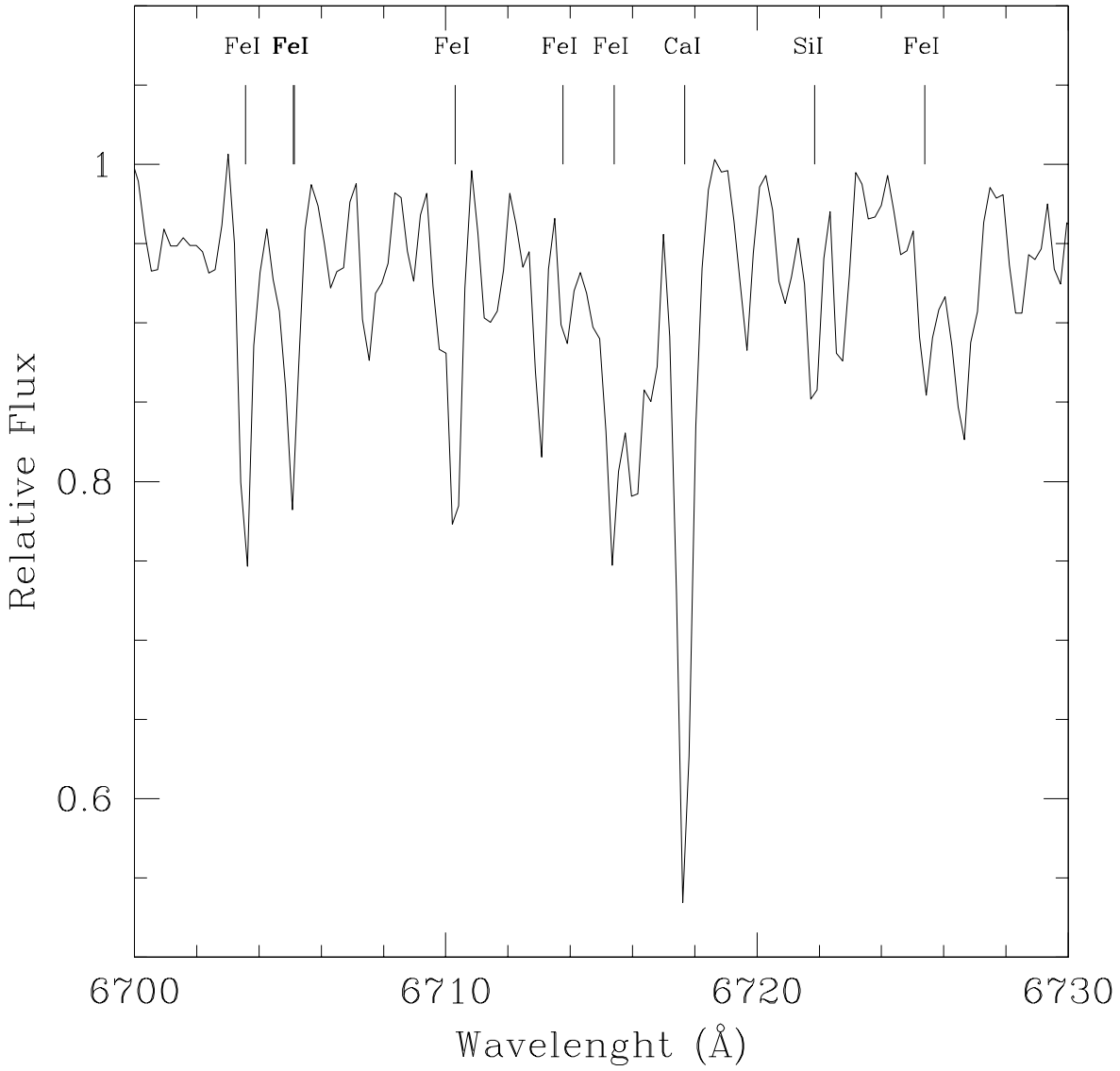

Fig. 2.— An example of extracted spectrum for the star #1181, with the main lines indicated.

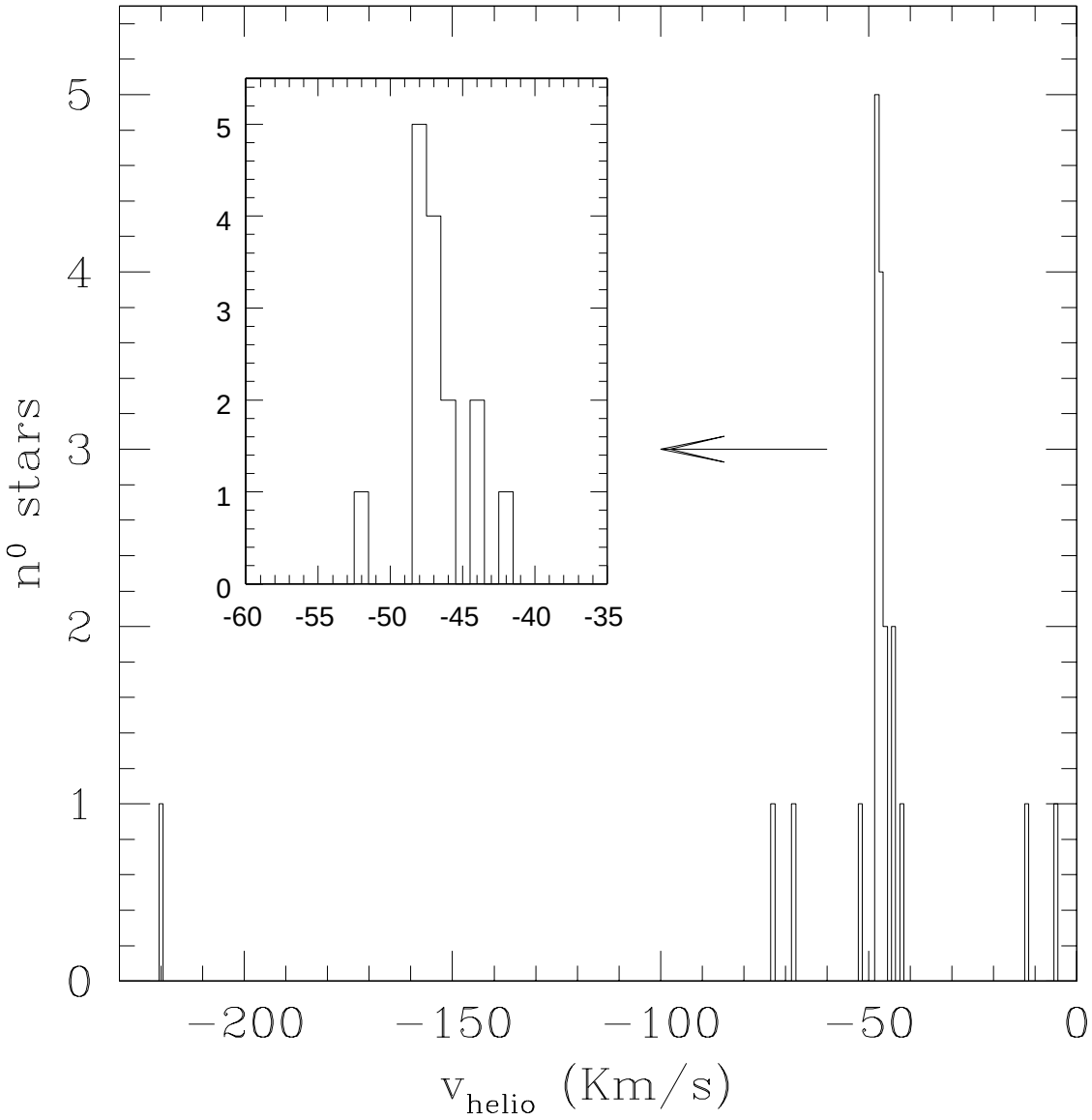

Fig. 3.— Radial velocity distribution of the 20 observed target stars.

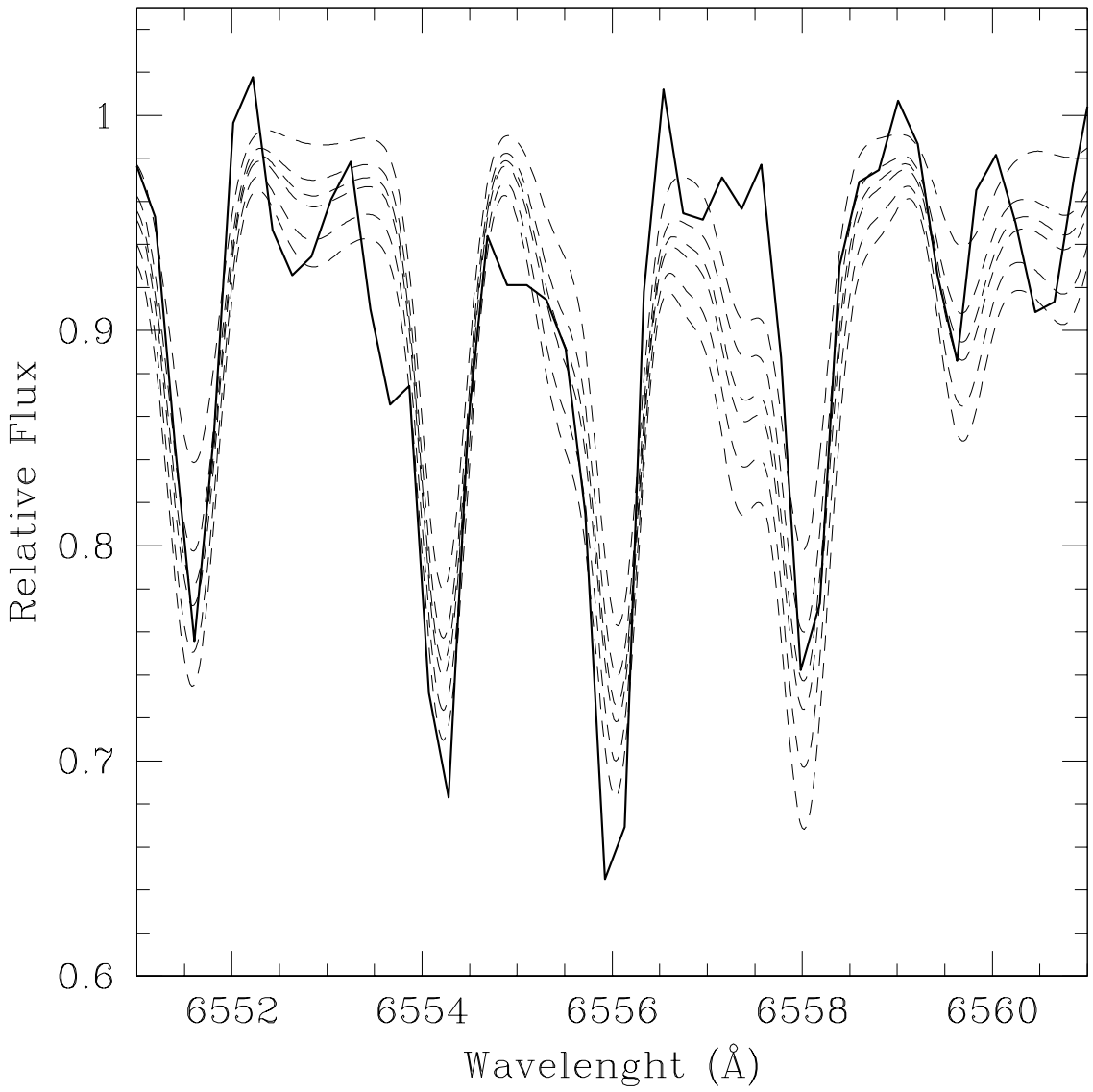

Fig. 4.— The spectrum of Fig 2. (thicker line) and a set of synthetic spectra for [M/H]= -0.2, 0.0, +0.2, +0.5 and +0.7, from the top to the bottom.

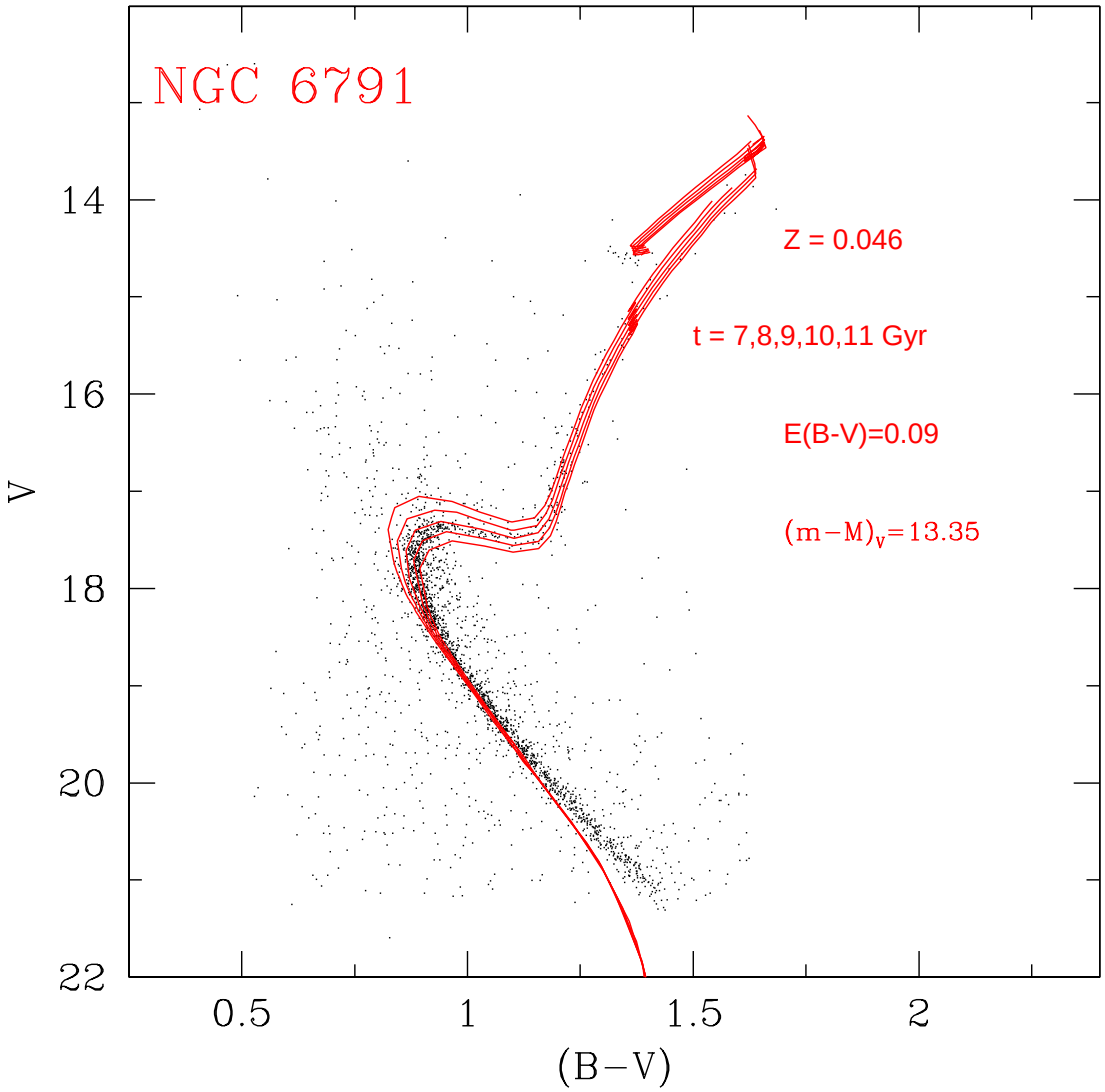

Fig. 5.— Five Padova isochrones for the ages of 7, 8, 9, 10, and 11 Gyr are fitted to the observed CMD in the V vs (B-V) plane. The isochrones are shifted by $E(B-V) = 0.09$ and $(m-M)_v = 13.35$.

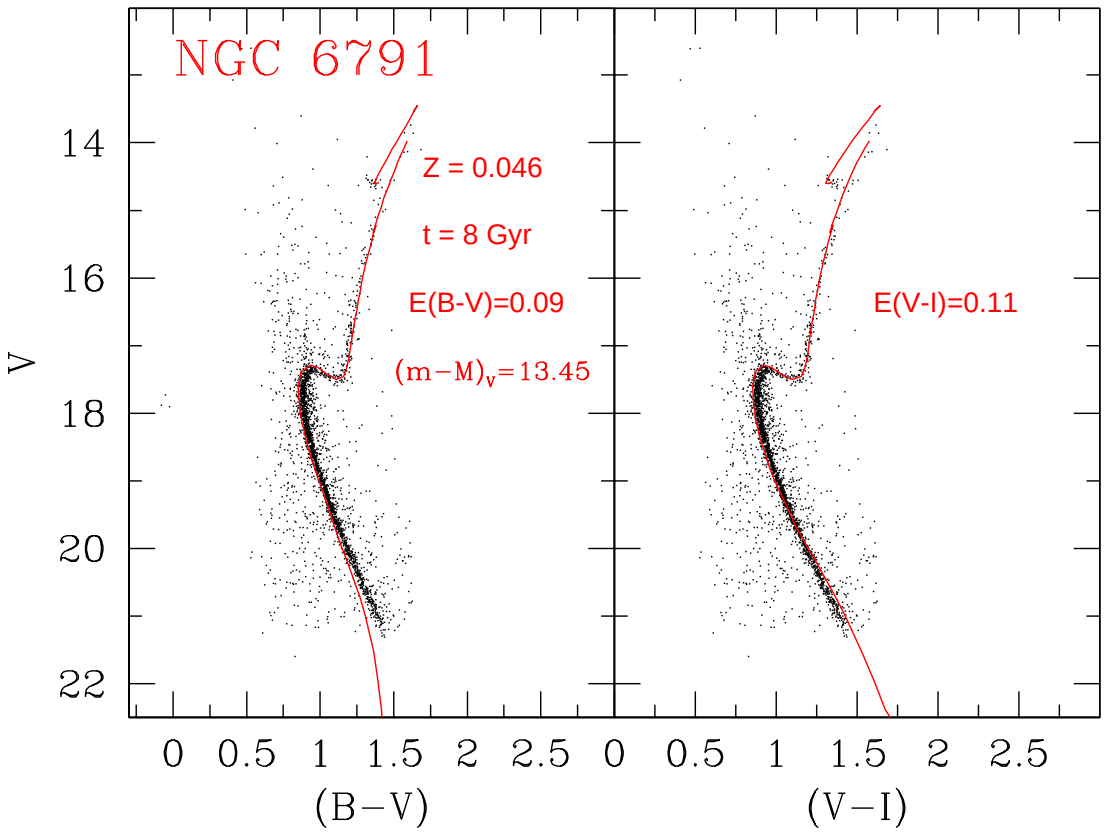

Fig. 6.— Best fit isochrone solution of the CMD of NGC 6791 with the Padova models. The isochrone and setting parameters are indicated in the plot.

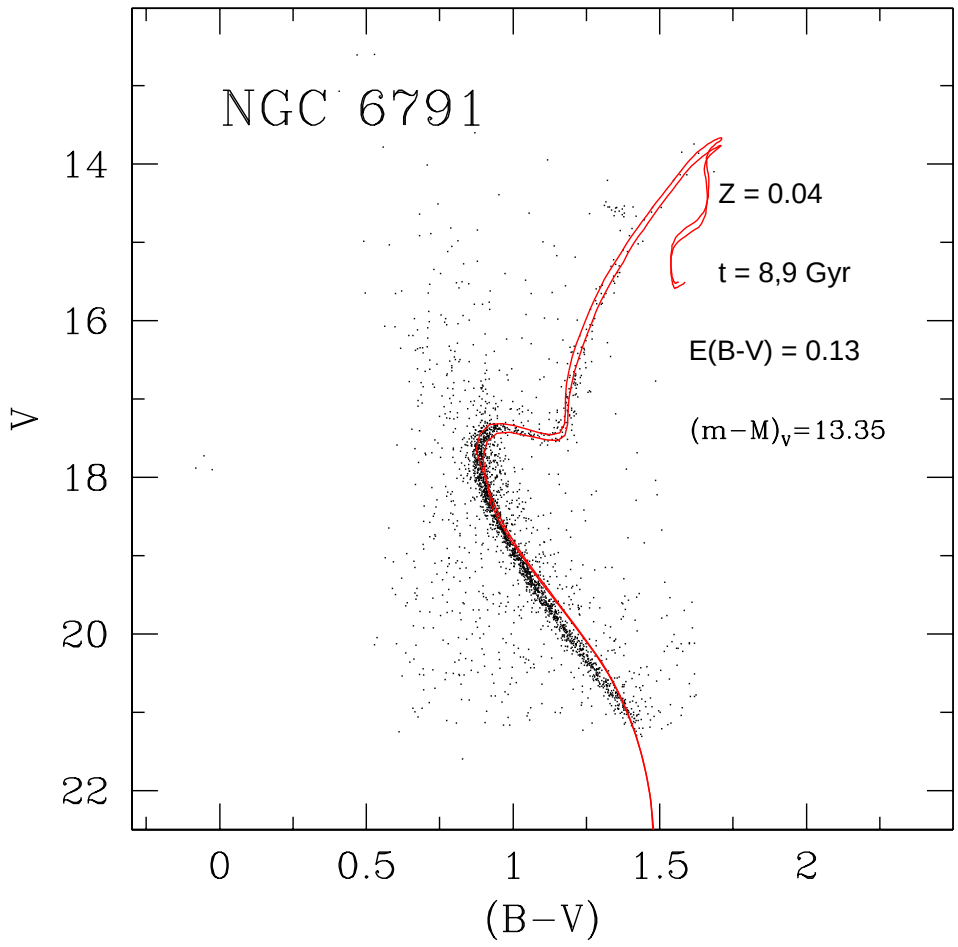

Fig. 7.— Yale-Yonsei isochrone solution for ages of 8 and 9 Gyr.

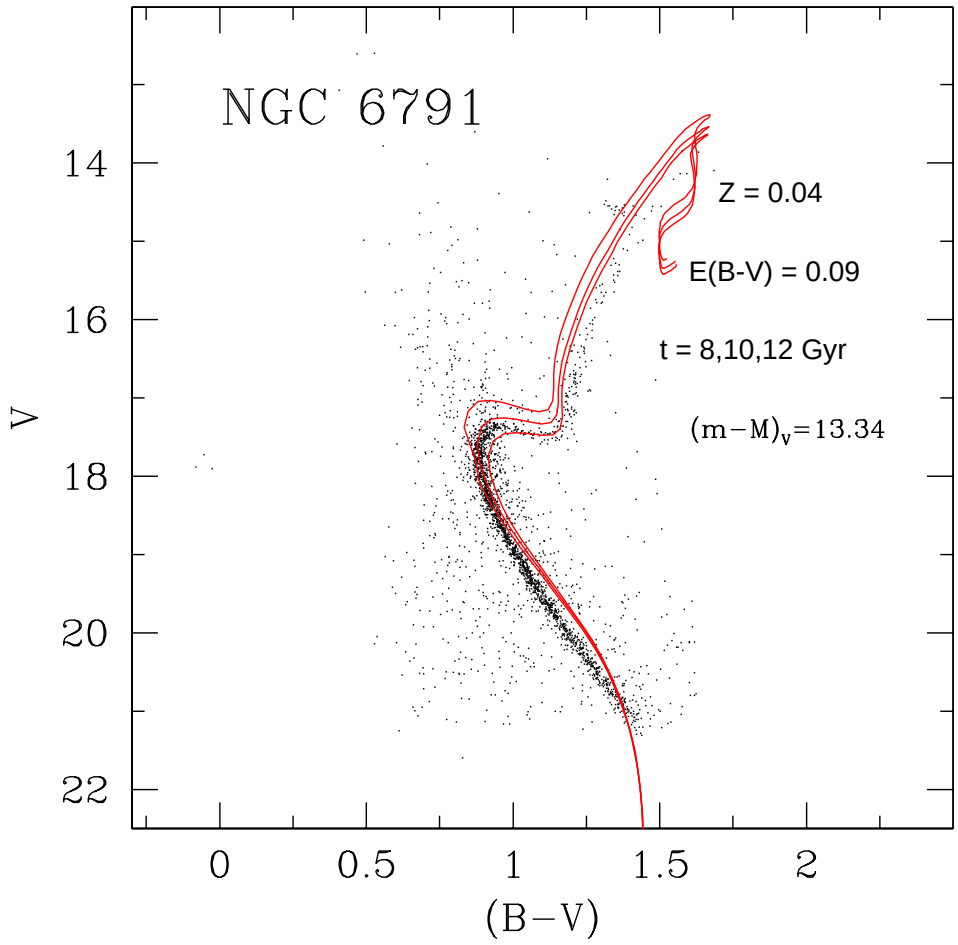

Fig. 8.— Yale-Yonsei isochrone solution for ages of 8, 10 and 12 Gyr (from the top to the bottom). Note how also the two older age isochrones are clealy ruled out.

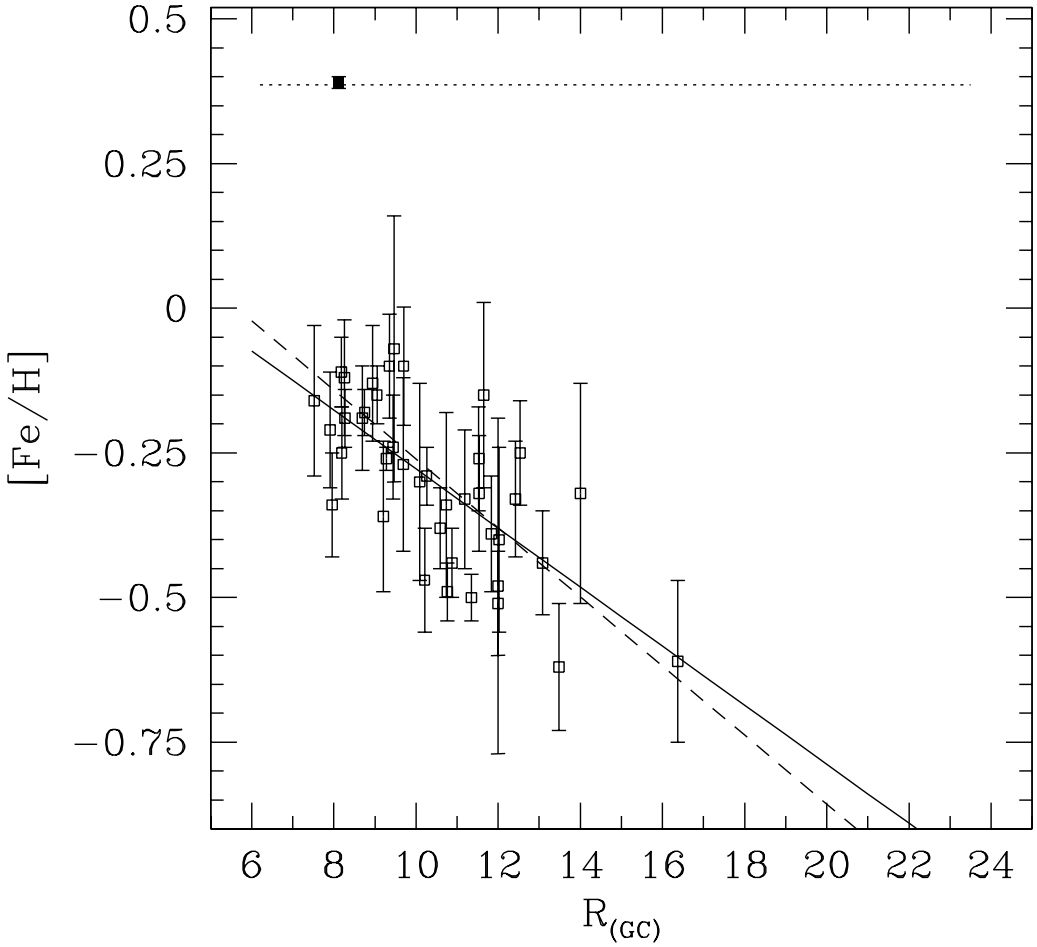

Fig. 9.— The Galactic disk chemical abundance radial gradient. The data are from Friel et al. (2002), with the exception of Berkeley 22 and Berkeley 66 taken from Villanova et al. (2005) and NGC 6791 (filled square, coming from the present study). The solid line is the linear fit without NGC 6791, whereas the dashed line is a linear fit to all the data points. The horizontal dotted line shows the epicyclical amplitude of NGC 6791 orbit.

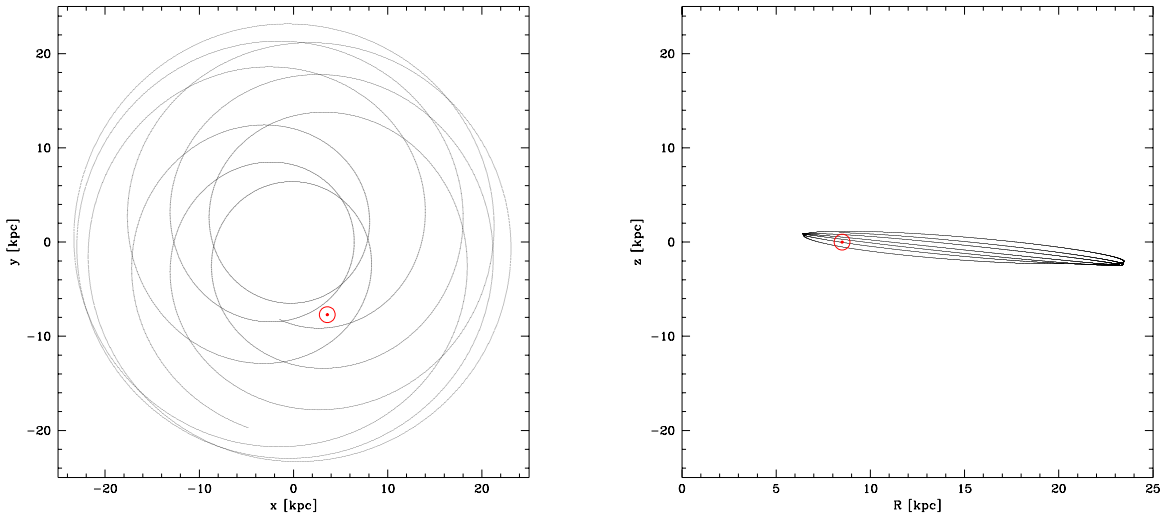

Fig. 10.— Galactic orbit of NGC 6791 in the X-Y and meridional plane. The position of the Sun is indicated.

Table 1. OBSERVED STARS

ID	K65	RA	DEC	V	(B-I)	V_{rad} (km s^{-1})	S/N	Spectral Type
10898		19:21:01.13	+37:42:13.80	14.459	3.059	-47.37±0.088	40	K4 III
11814	3003	19:21:04.27	+37:47:18.90	13.849	3.233	-46.52±0.082	60	K4/5 III
1442		19:21:16.33	+37:52:15.80	14.056	2.580	-11.84±0.056	100	
2044		19:20:30.92	+37:48:45.30	14.144	2.917	-5.27±0.072	40	
2423		19:20:33.26	+37:50:12.70	14.082	2.794	-220.41±0.066	70	
2793	3036	19:20:34.86	+37:46:30.10	14.538	2.751	-48.00±0.108	30	M1/2 III
3369	3030	19:20:37.89	+37:44:49.30	14.529	2.673	-48.37±0.094	40	K2/3 III
4162		19:20:40.85	+37:46:21.80	14.551	2.687	-52.11±0.146	10	K2/3 III
4715		19:20:42.73	+37:51:07.70	14.515	2.698	-47.91±0.088	50	K2/3 III
5583		19:20:45.58	+37:39:51.20	14.602	2.742	-43.62±0.196	10	K3/4 III
6940	3013	19:20:49.67	+37:44:08.00	14.588	2.659	-46.00±0.155	10	K2/3 III
7922		19:20:52.47	+37:50:15.80	14.482	2.671	-48.28±0.080	30	K2/3 III
7972	3010	19:20:52.60	+37:44:28.50	14.136	3.356	-44.35±0.094	40	K7 III
8082	SE-49	19:20:52.89	+37:45:33.40	14.546	2.639	-46.18±0.102	40	K2/3 III
8266	2001	19:20:53.39	+37:48:28.40	13.741	3.395	-47.73±0.080	40	K9 III
852		19:20:22.40	+37:51:42.40	14.738	2.748	-67.91±0.267	10	
8563		19:20:54.19	+37:46:28.80	14.554	3.071	-42.44±0.084	40	K4 III
8904	2008	19:20:55.11	+37:47:16.50	13.862	3.603	-46.91±0.098	30	M0 III
8988	3018	19:20:55.31	+37:43:15.60	14.557	3.005	-47.46±0.088	30	K4 III
95		19:20:11.19	+37:49:48.70	13.589	2.986	-72.93±0.076	50	

Table 2. ADOPTED ATMOSPHERIC PARAMETERS

ID	T_{eff} (^oK)	log g (dex)	v_t (km s^{-1})
10898	4100	2.53	1.0
11814	3980	2.17	1.1
2793	3760	2.02	1.1
3369	4400	2.79	1.0
4162	4370	2.78	1.0
4715	4360	2.76	1.0
5583	4300	2.75	1.0
6940	4400	2.81	1.0
7922	4390	2.77	1.0
7972	3920	2.23	1.1
8082	4410	2.81	1.0
8266	3900	2.04	1.2
8563	4080	2.55	1.0
8904	3830	2.01	1.2
8988	4130	2.60	1.0

Table 3. LINELIST

6408.016 FeI	6411.650 FeI	6419.980 FeI	6421.350 FeI	6436.430 FeI
6439.075 CaI	6449.808 CaI	6455.598 CaI		6464.661 FeI
6469.123 FeI	6469.210 FeI	6471.662 CaI		6481.880 FeI
6491.561 Ti2	6494.980 FeI	6496.897 BaII		6498.950 FeI
6499.650 CaI	6501.691 TiI	6518.380 FeI	6527.202 SiI	NiI
6554.230 TiI	6556.070 TiI	6569.230 FeI	6572.779 CaI	6574.240 FeI
6575.020 FeI	6581.221 FeI	6593.880 FeI	6606.970 TiII	6608.030 FeI
6609.120 FeI	6625.041 FeI	6627.560 FeI	6633.440 FeI	6633.760 FeI
6634.100 FeI	6643.640 NiI	6646.980 FeI	6663.231 FeI	6663.450 FeI
6677.955 FeI	6677.990 FeI	6698.673 AlI	6703.570 FeI	6705.101 FeI
6705.131 FeI	6710.310 FeI	6713.760 FeI	6715.410 FeI	6717.681 CaI
6721.848 SiI	6725.390 FeI	6733.160 FeI	6737.980 FeI	6741.628 SiI
6743.120 TiI	6743.185 TiI	6750.150 FeI		

Table 4. MEAN STELLAR ABUNDANCES

ID	[M/H]	[Fe/H]	[CaI/H]	[Ti/H]	[Ba/H]	[Si/H]	[Ni/H]	[Al/H]
10898	0.37±0.06	0.38±0.08	0.33±0.12	0.38±0.02		0.42	0.32	0.20
11814	0.39±0.09	0.34±0.08	0.32±0.08	0.34±0.05		0.39±0.03	0.29±0.14	0.23
3369	0.41±0.09	0.37±0.09	0.35±0.05	0.38±0.07	0.19	0.42	0.36	0.18
4715	0.39±0.07	0.36±0.05	0.33±0.07	0.35±0.02	0.18	0.41±0.02	0.42	0.23
7922	0.39±0.02	0.39±0.07	0.33±0.14	0.36±0.02		0.37±0.09	0.40	0.22
7972	0.40±0.09	0.39±0.05	0.35±0.06	0.34±0.05	0.20	0.39	0.41	0.26
8082	0.42±0.04	0.38±0.05	0.38±0.07	0.38±0.07	0.14	0.36	0.48	0.23
8266	0.37±0.05	0.37±0.05	0.38±0.07	0.37	0.24	0.39	0.31	0.19
8563	0.38±0.08	0.38±0.06	0.32±0.03	0.36±0.04	0.32	0.42	0.37	0.25
8988	0.36±0.06	0.40±0.07	0.35±0.10	0.31±0.07	0.22	0.39	0.34	

Table 5. ABUNDANCE RATIOS

ID	[Fe/H]	[Ca/Fe]	[Ti/Fe]	[Ba/Fe]	[Si/Fe]	[Ni/Fe]	[Al/Fe]
10898	0.38±0.08	-0.05	0.00		+0.04	-0.06	-0.18
11814	0.34±0.08	-0.02	0.00		+0.05	-0.05	-0.11
3369	0.37±0.09	-0.02	+0.01	-0.14	+0.05	-0.01	-0.19
4715	0.36±0.05	-0.03	-0.01	-0.15	+0.05	+0.06	-0.13
7922	0.39±0.07	-0.06	-0.03		-0.02	+0.01	-0.17
7972	0.39±0.05	-0.04	-0.05	-0.15	0.00	+0.02	-0.13
8082	0.38±0.05	0.00	0.00	-0.22	-0.02	-0.02	-0.15
8266	0.37±0.05	+0.01	0.00	-0.12	+0.02	+0.02	-0.18
8563	0.38±0.06	-0.06	-0.06	0.00	+0.04	-0.01	-0.13
8988	0.40±0.07	-0.05	-0.06	-0.13	-0.01	-0.01	